Special Issue: Powering the brain in health and disease

Astrocytic release of ATP through type 2 inositol 1,4,5-trisphosphate receptor calcium signaling and social dominance behavior in mice

Running title: Astrocytic ATP and social dominance

Guillot de Suduiraut Isabelle[1], Grosse Jocelyn[1], Ramos-Fernández Eva[1], Sandi Carmen[1] and Hollis Fiona[1,2#*]

[1]Brain Mind Institute, École Polytechnique Fédérale de Lausanne (EPFL), CH-1015 Lausanne, Switzerland

[2]Department of Pharmacology, Physiology and Neuroscience, University of South Carolina School of Medicine, Columbia, SC USA 29208

#Current Affiliation: Department of Pharmacology, Physiology and Neuroscience, University of South Carolina School of Medicine, Columbia, SC USA 29208

* To whom correspondence should be addressed:

Fiona Hollis
University of South Carolina School of Medicine
Columbia, SC USA 29208
Tel: +1 803 216 3514
Email: fiona.hollis@uscmed.sc.edu

Key Words: astrocytic ATP, social dominance, IP_3R2, type 2 inositol 1,4,5-triphosphate receptor, gliotransmission

Graphical Abstract

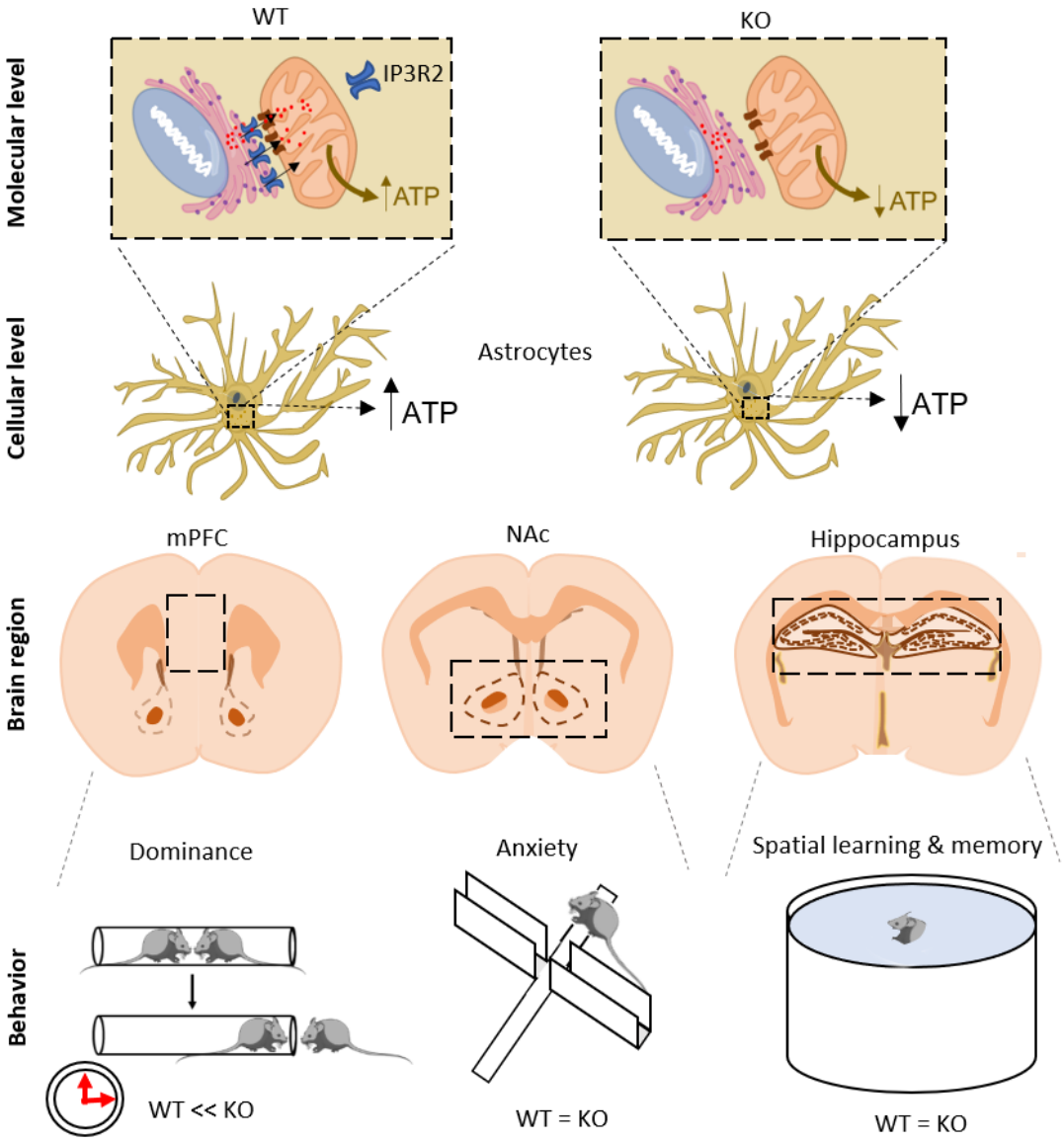

The role of aastrocytic ATP was investigated in social dominance using IP3R2 KO mice.

We found no differences between IP3R2 KO and WT mice in behavior or mitochondrial function

Astrocytic signaling through IP3R2 has a minimal role in social dominance behavior.

Abstract

Brain mitochondrial function is critical for numerous neuronal processes. We recently identified a link between brain energy and social dominance, where higher levels of mitochondrial function resulted in increased social competitive ability. The underlying mechanism of this link, however, remains unclear. Here we investigated the contribution of astrocytic release of adenosine triphosphate (ATP) through the type 2 inositol 1,4,5-triphosphate receptor to social dominance behavior. Mice lacking the type 2 inositol 1,4,5-triphosphate receptor were characterized for their social dominance behavior, as well as their performance on a nonsocial task, the Morris Water Maze. In parallel, we also examined mitochondrial function in the medial prefrontal cortex, nucleus accumbens, and hippocampus to investigate how deficiencies in astrocytic ATP could modulate overall mitochondrial function. While knockout mice showed similar competitive ability compared to their wildtype littermates, dominant knockout mice exhibited a significant delay in exerting their dominance during the initial encounter. Otherwise, there were no differences in anxiety and exploratory traits, spatial learning and memory, or brain mitochondrial function in either light or dark circadian phases. Our findings point to a marginal role of astrocytic ATP through IP_3R2 in social competition, suggesting that, under basal conditions, the neuronal compartment is predominant for social dominance exertion.

1. Introduction

Brain energy has been implicated in a variety of behavioral responses, including social behavior (Magistretti and Allaman, 2015). Mitochondria are organelles that produce energy in the form of adenosine triphosphate (ATP) via electron transport through a series of protein complexes called the electron transport chain. In the brain, mitochondria are located in areas of high demand to provide critical sources of ATP both in neurons and in glia (Ames, 2000). Neurons rely heavily on ATP production, primarily through oxidative phosphorylation (Belanger et al., 2011), and particularly at synapses, where even slight disruptions in ATP supply have drastic repercussions for cognitive function (Rangaraju et al., 2014). Astrocytes, the predominant glial cell in the central nervous system, are a main energy-producing cell type, releasing ATP in response to neuronal activity (Zhang et al., 2003). One of the main features in the communication between astrocytes and neurons is calcium (Ca^{2+}) signaling (Ding, 2013). Ca^{2+} may increase spontaneously or be triggered by endogenous or exogenous stimuli. There are several families of G-protein coupled receptors (GPCR) that can induce astrocytic Ca^{2+} release, including P2Y receptors, metabotropic glutamate receptors, and ɣ-aminobutyric acid b (GABAb) receptors (reviewed in Bazargani and Attwell, 2016). In astrocytes, the primary pathway for Ca^{2+} release from internal stores is via stimulation of GPCRs and subsequent activation of phospholipase C (PLC; reviewed in Bazargani and Attwell, 2016). PLC activation results in the release of inositol-1,4,5-trisphosphate (IP_3), which then binds to IP_3 receptors initiating Ca^{2+} release (reviewed in Bazargani and Attwell, 2016). Increases in astrocytic Ca^{2+} are reported to release transmitters that regulate neuronal and vascular function, including ATP (reviewed in Bazargani and Attwell, 2016).

Astrocytic release of ATP is now recognized as a form of gliotransmission that can modulate neuronal excitability and synaptic transmission (Halassa and Haydon, 2010; Volterra and Meldolesi, 2005). The importance of ATP gliotransmission for mental health has been suggested by Cao and colleagues (Cao et al., 2013), who identified a role for ATP released from astrocytes in stress-induced depressive-like behavior in mice (Cao et al., 2013), though its role in social behaviors is relatively unexplored (Petravicz et al., 2014). As disruption of astrocytic Ca^{2+} signaling has been implicated in numerous behaviors, including cognition, emotion, motor, and sensory procession (reviewed in Oliveira et al., 2015), astrocytic Ca^{2+} signaling may also be involved in social behavior. Understanding the contribution of astrocytic Ca^{2+} signaling and ATP release to social behavior can help in the development of future therapies for social deficits.

We previously identified a link between brain energy metabolism and social behavior. Specifically, we reported that highly anxious individuals exhibit reduced mitochondrial function in the Nucleus Accumbens (NAc) that is associated with lower levels of ATP and, ultimately, low competitive success during a social encounter against a low anxious conspecific (Hollis et al., 2018; Hollis et al., 2015; van der Kooij et al., 2018). Here, we aimed to examine the potential involvement of astrocytic ATP release in social competitive behavior using a genetic approach. ATP is released by astrocytes primarily through the aforementioned calcium-dependent activation of type 2 inositol-1,4,5-trisphosphate-receptor (IP_3R2) (Agulhon et al., 2012; Di Castro et al., 2011; Petravicz et al., 2008). The generation of *IP_3R2* knockout mice that consequently exhibit impaired ATP release, have allowed researchers to investigate the contribution

of astrocytic ATP to synaptic function and plasticity. Here, using an *IP_3R2* KO mouse model previously validated for its deficit in astrocytic ATP release (Cao et al., 2013), we assessed the functional role of IP_3R2 in social competition using the dominance tube test. In addition, we examined the impact of IP_3R2 in other behaviors including, anxiety, exploration and learning and memory. Finally, we analyzed whether deficiencies in astrocytic ATP could influence mitochondrial function in specific brain regions.

2. Materials and methods

2.1 Animals

One cohort of animals was group housed in standard plastic cages (19 X 27 X 13 cm) on a 12 h light/dark cycle (lights on at 07:00 h) in a pathogen-free facility. A separate cohort of animals was group housed on a reversed 12h dark/light cycle (lights on at 21:00 h) (data presented in Figure 5). Temperature and humidity in the animal housing room were maintained at 23 ±1 and 50% ±15%, respectively. Food and water were available to all animals *ad libitum*. All procedures described were conducted according to the Swiss National Institutional Guidelines of Animal Experimentation, with approval through a license issued by the Cantonal Veterinary Authorities (Vaud, Switzerland), and in accordance with the EU Directive 2010/63/EU. All efforts were made to minimize animal number and suffering during experiments. All efforts were made to comply with the ARRIVE guidelines for reporting animal experiments.

All experiments were conducted on adult (8-10 weeks of age) male IP_3R2-/- mice (KO) and their IP_3R2+/+ littermates (WT) derived from in-house breeding at the animal facility of the Ecole Polytechnique Federale de Lausanne (EPFL). The generation of these IP_3R2-deficient mice has been previously described (Li et al., 2005). Briefly, ES clones containing the IP3R2 targeting vector were microinjected into blastocysts from C57/Bl6J mice to generate chimeras which were subsequently bred with swiss mice generate germline transmitted floxed heterozygous mice. Mice were then intercrossed and crossed to Pro-Cre mice, and eventually IP3R2+/- mice to generate homozygous null mutant mice in a C57/Bl6J background (Li et al., 2005). Analysis of transgenic mice was performed by PCR on genomic DNA from ear biopsies. Primers against WT (forward, ACCCTGATGAGGGAAGGTCT; reverse, ATCGATTCATAGGGCACACC) and allele specific mutants (neo-specific primer: forward, AATGGGCTGACCGCTTCCTCGT;
reverse, TCTGAGAGTGCCTGGCTTTT) were used to genotype the animals. PCR products were visualized by ethidium bromide staining.

2.2 Behavioral analyses

We exposed KO and WT mice to the Elevated Plus Maze, Open Field, Novel Object test, social competition, and Morris Water Maze. All behavioral tests were performed between 09:00-14:00. For one cohort of animals, this meant that behavior was performed during the first half of the light cycle (data in figures 1-4). For a second cohort of animals reared in a reverse light cycle, this meant that behavior was performed in the first half of the dark cycle (data in figure 5). In all behavioral tests,

video-recording (MediaCruise, Canopus Co., Ltd., Kobe, Japan) was performed, and an automated-tracking system (Ethovision 11, Noldus IT) was used.

2.2.1 Elevated plus maze

To measure trait anxiety levels, mice were placed on an elevated plus maze apparatus, as described in Larrieu et al., 2017. The apparatus was made from black PVC with white inlays. The apparatus consisted of a central platform (5 × 5 cm) elevated from the ground (65 cm) with two open (30 × 5 cm) and two opposing (30 × 5 × 14 cm) close arms. Light conditions were maintained at 14–15 lux in the open arms, and 3–4 lux in the closed arms. At the start of the test, animals were placed in the central platform facing one of the closed arms. Animals were allowed to explore the apparatus for 5 min. The maze was cleaned with 5% ethanol after each trial.

2.2.2 Open field and Novel Object

We performed the open field test (OF) to investigate the animals' emotional and exploratory behavior at baseline conditions, as previously described in Larrieu et al., 2017. The OF consisted of a rectangular arena (50 × 50 × 40 cm) that was illuminated with dimmed lights (5–6 lx). Mice were introduced near the wall of the arena and allowed to explore for 5 min. Time spent in a virtual center zone (25 × 25 cm), was analyzed as an indicator of anxiety-like behavior.

Immediately following the OF, mice were subjected to the novel object reactivity test (NO). For this purpose, a small, plastic bottle was placed in the center of the open field while the mouse was inside. The mice were then given 5 min to freely explore the novel object. The time spent (s) in the center and the periphery of the compartment, total distance moved (cm) in the center and in the whole compartment were analyzed. The arena was cleaned with 5% ethanol in between each trial.

2.2.3 Social competition test

In order to assess social dominance behavior, mice were matched for weight and anxiety profile, and then separated into pairs according to genotype such that animals in each pair were with an opposite genotype (WT vs KO). The mice were pair-housed (WT with KO) for 16 days prior to the dominance tube test.

2.2.4 Dominance Tube test: We performed the dominance tube test as described in Wang et al., 2011. One transparent Plexiglas tube with 30 cm length and 3 cm inside diameter has been used. This diameter is a size just sufficient to allow our adult mice to pass through without reversing the direction. The test was given in two phases: a training phase and a test phase. During the training phase, each animal was given four trials on seven days. A trial consisted of releasing a mouse at one end of the tube and allowing it to run through the tube, sometimes with the help of a plastic stick pushing at its back. During the test phase: two mice were released simultaneously into the opposite ends and care was taken to ensure that they met in the middle of the tube. The mouse that first retreated from the tube within 2 minutes was designated the loser of the trial. Each pair was tested in three encounters during 3 consecutive days. Each mouse was ranked by their winning scores (between 0 and 3, with 3 indicating a win). Trials were scored by an individual blind to the genotypes.

2.2.5 Morris Water maze

Learning and working memory of the mice were assessed using the Morris Water Maze (MWM), as previously described (Conboy and Sandi, 2010). The apparatus consisted of a large white circular pool (140 cm in diameter) filled with opaque colored water. Mice were trained to locate a hidden platform located in the middle of one of the virtual quadrants with the help of extra-maze visual cues. The hidden platform (10 x 10 cm) was submerged 0.5 cm beneath the water surface and placed in a fixed location in the middle of one of the virtual quadrants. Both pool and platform were made of white polyvinyl plastic and offered no intra-maze cues to guide escape behavior. Mice were trained at 22˚C water temperature. The general experimental procedure was organized as follows. Mice received a pre-training session (day 1) followed by 3 days (days 2–4) of spatial training. The goal of the pre-training session was to habituate mice to the apparatus and water (22 ˚C). First, they were given a free swim trial (without platform) for 2 min. At the end of this trial, the platform was rapidly placed in the pool and the mouse allowed to stay on it for 15 s. After a 10 min intertrial interval, mice were given a 60 s training trial. Training was given over the subsequent 2–4 days. Each spatial training session consisted of six trials (intertrial interval 6 min). Each trial started with the mouse facing the wall at one of three possible start positions. If the mouse did not find the platform within 60 s, it was guided toward it. Each mouse remained on the platform for 15 s before being taken out and placed in a holding cage. Twenty-four hours after the last training session (i.e., day 5), memory was assessed through a 60 s probe test held without the platform.

Afterwards, the animals received a reversal learning. The platform was placed in the opposite quadrant compared to the first training phase. Reversal training was given over the subsequent 8–9 days. As in the first training session, each reversal training session consisted of six trials (intertrial interval 6 min). Each trial started with the mouse facing the wall at one of three possible start positions. If the mouse did not find the platform within 60 s, it was guided toward it. Twenty-four hours after the last training session (ie, day 10), memory was assessed through a 60 s probe test held without the platform.

2.3 Mitochondria Respirometry.

To measure mitochondrial function, animals were sacrificed under basal conditions at the same time of day as behavioral tests were performed by rapid decapitation and the nucleus accumbens, prefrontal cortex, and hippocampus were rapidly dissected out, weighed, and placed in a petri dish on ice with 2 mL of relaxing solution (2.8 mM Ca2K2EGTA, 7.2 MK2EGTA, 5.8 mM ATP, 6.6 mM MgCl2 , 20 mM taurine, 15 mM sodium phosphocreatine, 20 mM imidazole, 0.5 mM dithiothreitol and 50 mM MES, pH = 7.1) until further processing.
Tissue samples were then gently homogenized in ice cold respirometry medium (MiR05: 0.5 mM EGTA, 3mM $MgCl_2$, 60 mM potassium lactobionate, 20 mM taurine, 10 mM KH2 PO4, 20 mM HEPES, 110 mM sucrose and 0.1% (w/v) BSA, pH=7.1) with an eppendorf pestle. Then, 2 mg of tissue were used to measure mitochondrial respiration rates at 37°C using high resolution respirometry (Oroboros Oxygraph 2K, Oroboros Instruments, Innsbruck, Austria), as previously described (Hollis et al., 2015).

A multi-substrate protocol was used to sequentially explore the various components of mitochondrial respiratory capacity (including assessments of complex I, complex I and II, maximum capacity, and complex II respiration). Residual oxygen consumption (ROX) due to non-mitochondrial respiration was measured and subtracted from all other substrate measurements. All respiration experiments comprise 2-3 counterbalanced blocks across days.

2.4 ATP quantification

Freshly dissected prefrontal cortex, nucleus accumbens, and hippocampus were placed in 2mL of relaxing solution on ice. Tissue samples were then diluted 10x in a tricine buffer solution (40 mM Tricine, 3 mM EDTA, 85 mM NaCl, 3.6 mM KCl, 100 mM NaF and 0.1% saponin, pH 7.4; Sigma Aldrich). ATP content was determined enzymatically with luciferase in a white 96-well plate. In the presence of ATP, Mg^{2+} and oxygen, luciferin is oxygenated by luciferase into oxyluciferin. This reaction emits light which is proportional to the amount of ATP in the sample. ATP was measured with the CellTiter-Glo Luminescent Cell Viability Assay (Promega), with a few minor modifications. A converting solution (100 mM Tricine, 100 mM $MgSO_4$, 25 mM KCl) was added to tissue samples and allowed to incubate at room temperature for 5 min. After incubation, a $MgCl_2$ solution (4 mM tricine and 100 mM $MgCl_2$) was added to the samples, followed by, 35 µl of CellTiter-Glo reagent (G7571, Promega). Additionally, each 96-well plate contained a series of 10-fold dilutions (1µM – 10nM) of an ATP standard (Sigma), in order to generate a standard curve for each assay. Luminescence was immediately detected with a luminometer (Safire 2, Tecan). Luminescence was measured kinetically via 40 cycles taken at 1 min intervals. At least 4 points at the steady-state were taken to generate an average maximum luminescence for each sample. ATP was calculated using the standard curve to determine the concentration of ATP.

2.5 Statistical Analyses

Normality of data was verified using D'Agostino and Pearson normality tests. Anxiety and exploratory data were analyzed by unpaired t-tests or, when nonparametric, by Mann-Whitney tests. Dominance tube test data were analyzed by one sample t-tests against hypothetical chance values and repeated measures ANOVAs. Respirometry and ATP experiments were performed in counterbalanced experimental blocks and analyzed using a linear mixed model including a random effect of block. Respirometry data are presented as estimated marginal meas. Morris water maze data were analyzed by unpaired t-tests and repeated measures ANOVA. All data other than respirometry data represent group means with standard error, with one mouse equal to one data point. With the exception of respirometry data, all data were analyzed using Prism version 7 (Graphpad software Inc, San Diego, CA). Mitochondrial respirometry data were analyzed using SPSS statistical software version 21.0 (SPSS, Chicago, IL). Sample sizes for each experiment were based on previous and/or pilot experiments and are indicated in the text and figure legends.

3. Results

As inherent traits can influence the outcome of a social competition (Hollis et al., 2018; Hollis et al., 2015; van der Kooij et al., 2018), we first characterized wildtype (WT) and *IP$_3$R2-/-* (KO) mice for natural anxiety and exploration. We found no significant differences in the percentage of time spent in the open arms (Mann-Whitney test, U=88.5; p=0.48), number of entries (unpaired t-test; t=0.78; p=0.45) or distance traveled (unpaired t-test, t=0.22; p=0.82) in the elevated plus maze between WT and KO littermates (Figure 1A-D; n=14-15/group). Similarly, we also found no significant differences in the time spent in the center (Mann-Whitney test, U=90; p=0.53), number of center entries (unpaired t-test, t=0.86, p=0.40), or distance moved (unpaired t-test, t=0.75, p=0.46) in the open field (Figure 1E-H; n=14-15/group). Animals were also assessed for their exploratory behavior in the novel object reactivity test, where there were no differences in time spent in the center zone with the object (Mann-Whitney test, U=102, p=0.91), number of entries (Mann-Whitney test, U=104.5, p=0.99), or distance traveled (unpaired t-test, t=0.58, df=27, p=0.57; Supplementary Figure 1A-C; n=14-15/group).

To evaluate social dominance behavior, *IP$_3$R2-/-* mutants were pair-housed with a wildtype mouse of similar anxiety and weight. Following two weeks of cohabitation (including one week of habituation and one week of training), the social hierarchy of the pair was tested in the tube test across multiple days (Figure 2A; n=14 WT-KO pairs). Overall, we found that within a pair, the hierarchy could be detected and was stable across testing days. Across all sessions, KO animals exhibited an equal probability to become dominant (one-sample t-test t=0.59; df=13; *p*=0.57; Figure 2B). When considering the competition across the three testing days, there was no significant effect of genotype (RM-ANOVA, F(1,26)= 0.69; p=0.41), time (F(2,52)= 0.0004; p=0.99) or an interaction (F(2,52)= 2; p=0.15; Figure 2C). Dominant mice exhibited a significant decrease in their latency to push the subordinate mouse out of the tube (F(3.2, 19.4)= 4.51; p = 0.01; Figure 2D). While there was no significant effect of genotype (F(1,6)=0.66; p =0.44), during the testing phase, there was a significant interaction between genotype and day ((F(8,48)=5.05; p= 0.0001) such that dominant KO mice took longer to push the subordinate out of the tube compared to dominant WT mice (Figure 2D). Post-hoc tests indicated that this effect was driven by a trend only present on the first trial of the first day. Overall, these data suggest that astrocytic ATP released through the type 2 IP_3 receptor is not responsible for the predisposition to a particular social rank, though there may be some contribution during the first establishment phase.

Given our previous finding linking mitochondrial respiration in the nucleus accumbens and social competitive ability (Hollis et al., 2015; van der Kooij et al., 2018), we explored whether astrocytic ATP influenced accumbal mitochondrial respiration. In the nucleus accumbens, *IP$_3$R2-/-* mice showed similar levels of both coupled (Figure 3A, CI: (F(1,23)=0.242; *p*=0.63, CI+CII: F(1,23.2)=0.204; *p*=0.67; n=14-15/group) and uncoupled (Figure 3A; ETS: F(1,23.2)=0.080; *p*=0.78, ETSCII: F(1,23.2)= 0.68; *p*=0.42; n=14-15/group) respiration through complexes I and II compared to WT littermates. Synaptic activity in the medial prefrontal cortex has been implicated in the establishment of social dominance, specifically for the dominance tube test (Wang et al., 2011; Zhou et al., 2017). Moreover, we recently identified an association between social competition and mitochondrial respiration in the medial prefrontal cortex (Hollis

et al., 2018). Thus, we examined mitochondrial respiration in this region as well. However, again, there were no significant genotypic differences in either coupled (CI: F(1,24.3)= 0.725 *p*=0.40, CI+CII: F(1,24.04)= 0.645; *p*=0.43; n=14-15/group) or uncoupled (ETS: F(1,22.57)= 0.397; *p*=054, ETSCII; F(1,24.01)= 0.162; *p*=1.0; n=14-15/group) respiration (Figure 3B).

As the dominance tube test is a social task, we tested whether astrocytic ATP release through IP3 type 2 receptors might influence behavior in a nonsocial task. Astrocytes have been implicated in learning and memory (Suzuki et al., 2011) and IP_3R2-mediated release of ATP is reported to be critical to the underlying synaptic hippocampal function (Pascual et al., 2005). As such, we examined performance in a hippocampal-dependent task, the Morris Water Maze (MWM; (Eichenbaum et al., 1990; Morris, 1981). The MWM is a task in which animals learn to find a hidden escape platform located in a specific quadrant of a circular arena with the aid of external visual cues. Both genotypes demonstrated similar abilities to learn the location of the platform during the training session as evidenced by a significant effect of time in the latency to escape the water (F(1, 12) = 0.3561; p=0.56; n=7/group; Figure 4A), and similar path lengths and velocities (Supplementary Figure 2A-B). During the probe trial, KO and WT littermates successfully recalled the location of the hidden platform, each spending significantly more time in the goal quadrant than chance levels (WT: t=7.37 df=6; p=0.0002; KO: t= 4.81, df=6; p=0.003; n=7/group; Figure 4B-C). There were no significant differences in the time spent in the goal quadrant between WT and KO mice (t= 0.125; df=12; p= 0.90; Figure 4C). Immediately following the probe trial, the mice were subjected to reversal learning. KO and WT littermates showed similar abilities to learn the new placement of the platform (t=0.01948 df=12; p=0.98; n=7/group; Figure 4A days 8-9). During the reversal probe trial, both genotypes successfully extinguished the memory of the initial platform location but did not recall the new location, spending similar amounts of time in each quadrant during the probe (t=0.03632 df=6; p=0.97; n=7/group; Figure 4D) to a similar degree. This data suggests that astrocytic release of ATP by IP_3R2 does not mediate learning or memory in a spatial task. As the MWM is a hippocampal-dependent task, we also examined hippocampal mitochondrial function. Again, we found no significant differences between WT and KO mice in coupled (F(1,8.9)=2.6; p=0.14; CI+CII: F(1,8.9)=2.8; p=0.13) or uncoupled (ETS: F(1,8.9)=3.1; p=0.11; ETSCII: F(1,8.9)=2.4; p=0.16) respiration (Figure 4E; n=4-9/group).

Astrocytic ATP release through the type 2 IP3 receptor is circadian (Womac et al., 2009; Marpegan et al., 2011) and antiphasic to neuronal peak levels (Brancaccio et al., 2017). As we performed our behavioral and molecular tasks at the same time during the circadian day, one potential explanation for our lack of effects was the timing of the experiments. To address this, we repeated behavioral and mitochondrial experiments in a separate cohort of animals during the circadian night, when astrocytic ATP release is at its peak (Womac et al., 2009; Marpegan et al., 2011). During the dark phase, we found no significant differences in the percentage of time spent in the open arms (Mann-Whitney test, U=32; p>0.99), number of entries (unpaired t-test; t=1.08; df=14; *p*=0.30) or distance traveled (unpaired t-test; t=0.67; df=14; *p*=0.52) in the elevated plus maze between WT and KO littermates (Figure 5A-C; n=8/group). When animals were tested for their social dominance behavior in the dominance tube test, *IP_3R2-/-* animals exhibited an equal probability to become dominant (one-sample t-test t=0.23; df=7; *p*=0.84; Figure 5D; n=8 WT-KO pairs). Moreover, across the three

testing days, there was no significant effect of genotype ($F(1,14)=0.082$; $p=0.78$), time ($F(1.82, 25.5)=1.06e-12$; $p>0.99$) or an interaction in the number of trials won ($F(2,28)=0.64$; $p=0.53$; Figure 5E; n=8/group). Finally, unlike our testing in the light phase, there were no significant differences in the time to exert dominance between dominant KO and WT mice (Figure 5F; n=4/group) at the genotype ($F1,6)=1.69$; $p=0.24$), time ($F(2.2, 13.7)=2.1$; $p=0.16$), or interaction ($F(8,48)=1.4$; $p=0.21$) levels. We also analyzed mitochondrial respiration in the three previously measured brain regions. As before, we found no significant differences between KO and WT mice in the nucleus accumbens (CI: $F(1,11)=0.004$; $p=0.95$; CI+CII: $F(1,14)=0.064$; $p=0.80$; ETS: $F(1,14)=0.024$; $p=0.88$ ETSCII: $F(1,14)=0.026$; $p=0.88$; Figure 5G; n=8/group), prefrontal cortex (CI: $F(1,11)=0.34$; $p=0.57$; CI+CII: $F(1,11)=0.016$; $p=0.90$; ETS: $F(1,11)=0.56$; $p=0.47$; ETSCII: $F(1,11)=0.29$; $p=0.60$; Figure 5H; n=8/group), or hippocampus (CI: $F(1,11)=0.69$; $p=0.43$; CI+CII: $F(1,11)=0.74$; $p=0.41$; ETS: $F(1,11)=0.61$; $p=0.45$; ETSCII: $F(1,11)=0.88$; $p=0.37$; Figure 5I; n=8/group). Finally, as the major output of mitochondrial function is ATP production, we measured total levels of ATP in brain tissue homogenates. Here we found no significant differences in ATP levels in the prefrontal cortex ($F(1,11)=2.1$; $p=0.18$; Figure 5J; n=8/group), nucleus accumbens ($F(1,14)=0.086$; $p=0.77$; Figure 5K n=8/group) or hippocampus ($F(1,9.9)=1.34$; $p=0.27$; Figure 5L; n=8/group), suggesting that global levels of ATP were unaffected by elimination of IP_3R2.

4. Discussion

Here, we investigated the contribution of astrocytic ATP release via IP_3 type 2 receptors to social dominance behavior using a genetic approach with the *IP_3R2-/-* mice that reportedly lack the Ca^{2+} signaling required for ATP release. Mutant mice did exhibit a significant delay during the initial encounter during light cycle testing, suggesting that astrocytic IP_3R2 release of ATP may partially contribute to the first establishment phase of a social competition, but have no further bearing on the outcome of subsequent competitions. Interestingly, this initial delay was not seen when social dominance was tested in the dark cycle during peak astrocytic ATP release, suggesting a mild circadian influence on IP_3R2-mediated ATP release in social hierarchy assertion. Taken together, our data point to a minimal role for IP_3R2 astrocytic release of ATP in social dominance assertion, with mutant mice exhibiting similar capabilities in the dominance tube test as their wildtype littermates across three testing days. This lack of overall impact of IP_3R2-mediated astrocytic ATP release on the home cage social hierarchy supports and extends our previous work, where examination of c-FOS activation following social dominance revealed activation of neuronal, but not astrocytic cells (Hollis et al., 2015).

We have previously identified links between social dominance and mitochondrial respiration in the nucleus accumbens (Hollis et al., 2015; van der Kooij et al., 2018), and the prefrontal cortex (Hollis et al., 2018). Here, we investigated whether astrocytic ATP release would impact mitochondrial function in these brain regions. In line with our behavioral results, we did not see any significant differences between WT and KO mice in mitochondrial respiration in either the nucleus accumbens or prefrontal cortex. This result is in line with our previous finding, where inherent differences in social competition were linked to mitochondrial respiration in the neuronal, but not glial compartment of nucleus accumbens tissue (Hollis et al., 2015). The prefrontal cortex

has also been heavily implicated in social hierarchy, consistently at the neuronal level (Zhou et al., 2018). Indeed, manipulation of specific prefrontal cortical circuits at the synaptic level directly influenced social rank (Wang et al., 2011) and effortful competitive behavior (Zhou et al., 2017). While the literature thus far has not ruled out astrocytic involvement in social dominance behavior, our results further support a neuronal mechanism.

In addition to social dominance, we also compared basal behavioral traits between genotypes to determine if there were genotypic differences directly related to anxiety or exploratory behaviors. A lack of IP_3R2-mediated ATP, however, had no bearing on any of the traits that we measured. Moreover, we also observed similar capabilities in the Morris Water Maze, during both learning and reversal stages, minimizing the role of astrocytic ATP in spatial learning and memory. These findings are in agreement with others, who have also noted no differences between IP_3R2 WT and KO mice (in IP_3R2 both conditional and constitutive mutants) in behavior on the elevated plus maze, open field, or Morris Water Maze (Bonder and McCarthy, 2014; Petravicz et al., 2014; Takata et al., 2013). Initial reports described alterations in long-term potentiation both *in vitro* (Gordon et al., 2005; Newman, 2003; Pascual et al., 2005; Serrano et al., 2006; Zhang et al., 2003) and *in vivo* (Navarrete et al., 2012; Wang et al., 2012), though several groups have found no genotypic differences at the synaptic level (Agulhon et al., 2010; Fiacco et al., 2007; Petravicz et al., 2008), leaving the importance of astrocytic ATP release unclear. Our data add further reinforce the idea that IP_3R2-mediated ATP release is not necessary for hippocampal-dependent learning, or other limbic-associated behaviors.

Given the energy demands imposed by stress (Picard et al., 2018), animals under a higher allostatic load might show impairments while those under non-stressed conditions might not. Indeed, we have found that stress can identify impairments in decision-making that were previously undetected under baseline conditions (Goette et al., 2015). Furthermore, Cao and colleagues previously identified an intriguing link between ATP gliotransmission through IP_3 type 2 receptors and stress-induced depressive-like behaviors (Cao et al., 2013). Our investigations were performed in two tasks previously reported to induce stress – a social dominance competition (the dominance tube test; (Sapolsky, 2005)) and a spatial learning test (the Morris Water Maze; MWM; (Conboy and Sandi, 2010)). If astrocytic ATP release through IP_3 type 2 receptors provides an important source of modulation to neuronal function, then under stressful conditions, animals lacking such energy sources should show deficits. As the KO mice performed at similar levels to WT littermates under both psychological or physical stress, we can rule out, to a large extent, stress as a modifying factor.

It is important to emphasize the complexity of astrocytic function, with calcium fluctuations occurring at different compartments of the astrocyte with different modes of activation and fluctuations at frequencies that are challenging to capture with our current technology (Bindocci et al., 2017; Savtchouk and Volterra, 2018; Volterra et al., 2014). Thus, we cannot exclude that there may be an additional source of astrocytic ATP aside from the IP_3 receptor. Indeed, we were unable to detect a difference in global ATP measurements between KO and WT mice. It should be noted that our measurements were in tissue homogenates that also include neuronal ATP stores that may mask astrocyte-specific differences. The presence of local sources of ATP that were available in an IP_3R2-independent manner may also explain the lack of observable differences between wildtype and mutants. Indeed, recent studies found

that calcium fluctuations were not completely abolished in IP_3R2 mutant mice, but substantially decreased in the soma while nearly 40% of calcium fluctuations were still operating at local fine astrocytic processes (Agarwal et al., 2017; Srinivasan et al., 2015). These reports point to major differences in Ca2+ signaling between astrocytic compartments and suggest that IP_3R2 knockout mainly affects the astrocytic soma and leaves the processes intact. It should be noted however, that while calcium activity was still detected, application of ATP agonists in IP_3R2 mutant mice was unable to generate a detectable calcium response (Agarwal et al., 2017; Fiacco and McCarthy, 2018). This finding suggests that astrocytic release of ATP is impaired in these mutants (Agarwal et al., 2017; Fiacco and McCarthy, 2018), though mitochondrial activity at the fine processes may lead to ATP production to compensate. Indeed, a recent report found that Ca^{2+} signaling was still present at the endoplasmic reticulum of IP3R2 KO mice and allowed for privileged Ca^{2+} transfer to nearby mitochondria (Okubo et al., 2018). Whether this local ATP production is actually the necessary component in mediating mitochondrial and behavioral responses will be an important aspect for future studies.

ATP has been consistently highlighted as a critical source of energy for behavior (Mergenthaler et al., 2013). While the role of astrocytic gliotransmission in modulating synaptic activity and behavior is contested in the field, our findings suggest that astrocytic signaling through the IP_3R2 receptor has little to no bearing on social dominance behavior. Interestingly, IP_3R2 signaling also does not appear to play a critical role in the associated energy required at basal levels to sustain mitochondrial respiration within specific brain regions critical for this behavior. Instead our data reinforce the importance of neuronal ATP sources for complex behaviors, such as social dominance as well as learning and memory.

Acknowledgments

We thank Dr. J. Chen for the IP_3R2 mice and Olivia Zanoletti for her technical support. This work has been supported by grants from the European Union's Seventh Framework Program for research, technological development and demonstration under grant agreement no. 603016 (MATRICS), the Swiss National Science Foundation (31003A-152614, 31003A-176206, and NCCR Synapsy grant No. 51NF40-158776), and intramural funding from the EPFL to CS. FH was supported by a Marie-Heim Vögtlin fellowship from the Swiss National Science Foundation. The funding sources had no additional role in study design, in the collection, analysis and interpretation of data, in the writing of the report or in the decision to submit the paper for publication. This paper reflects only the authors' views and the European Union is not liable for any use that may be made of the information contained therein.

Author Contributions

FH and CS conceived and designed the study and wrote the manuscript. IGdS performed behavioral experiments, JG and ER provided technical support. FH, ER, and IGdS analyzed the data. ER design the graphical abstract. CS obtained funding and supervised the study. All authors have approved the final version of the manuscript.

Conflicts of Interest

The authors report no conflicts of interest.

Data statement

Access to the dataset in this study can be obtained by following a formal request procedure to the corresponding author.

Supplementary Materials

Supplementary material for this paper can be found at the journal website: https://onlinelibrary.wiley.com/journal/14609568

Abbreviations

ATP: adenosine triphosphate
Ca^{2+}: calcium
GABAb: gamma.aminobutyric acid receptor b
GPCR: G-protein coupled receptor
HPC: hippocampus
IP_3R2: type 2 inositol 1,4,5-triphosphate receptor
KO: knockout
MWM: Morris Water Maze
NAc: nucleus accumbens
NO: novel reactivity test
OF: open field test
PFC: prefrontal cortex
PLC: phospholipase C
WT: wildtype

References

Agarwal, A., Wu, P. H., Hughes, E. G., Fukaya, M., Tischfield, M. A., Langseth, A. J., Wirtz, D., Bergles, D. E., 2017. Transient Opening of the Mitochondrial Permeability Transition Pore Induces Microdomain Calcium Transients in Astrocyte Processes. Neuron 93, 587-605 e587.

Agulhon, C., Fiacco, T. A., McCarthy, K. D., 2010. Hippocampal short- and long-term plasticity are not modulated by astrocyte Ca2+ signaling. Science 327, 1250-1254.

Agulhon, C., Sun, M. Y., Murphy, T., Myers, T., Lauderdale, K., Fiacco, T. A., 2012. Calcium Signaling and Gliotransmission in Normal vs. Reactive Astrocytes. Front Pharmacol 3, 139.

Ames, A., 3rd, 2000. CNS energy metabolism as related to function. Brain Res Brain Res Rev 34, 42-68.

Bazargani, N. and Attwell, D., 2016. Astrocyte calcium signaling: the third wave. *Nature neuroscience*, *19*(2), p.182.

Belanger, M., Allaman, I., Magistretti, P. J., 2011. Brain energy metabolism: focus on astrocyte-neuron metabolic cooperation. Cell Metab 14, 724-738.

Bindocci, E., Savtchouk, I., Liaudet, N., Becker, D., Carriero, G., Volterra, A., 2017. Three-dimensional Ca(2+) imaging advances understanding of astrocyte biology. Science 356.

Bonder, D. E., McCarthy, K. D., 2014. Astrocytic Gq-GPCR-linked IP3R-dependent Ca2+ signaling does not mediate neurovascular coupling in mouse visual cortex in vivo. J Neurosci 34, 13139-13150.

Cao, X., Li, L. P., Qin, X. H., Li, S. J., Zhang, M., Wang, Q., Hu, H. H., Fang, Y. Y., Gao, Y. B., Li, X. W., Sun, L. R., Xiong, W. C., Gao, T. M., Zhu, X. H., 2013. Astrocytic adenosine 5'-triphosphate release regulates the proliferation of neural stem cells in the adult hippocampus. Stem Cells 31, 1633-1643.

Conboy, L., Sandi, C., 2010. Stress at learning facilitates memory formation by regulating AMPA receptor trafficking through a glucocorticoid action. Neuropsychopharmacology 35, 674-685.

Di Castro, M. A., Chuquet, J., Liaudet, N., Bhaukaurally, K., Santello, M., Bouvier, D., Tiret, P., Volterra, A., 2011. Local Ca2+ detection and modulation of synaptic release by astrocytes. Nat Neurosci 14, 1276-1284.

Ding, S., 2013. In vivo astrocytic Ca2+ signaling in health and brain disorders. *Future neurology*, *8*(5), pp.529-554.

Eichenbaum, H., Stewart, C., Morris, R. G., 1990. Hippocampal representation in place learning. J Neurosci 10, 3531-3542.

Fiacco, T. A., Agulhon, C., Taves, S. R., Petravicz, J., Casper, K. B., Dong, X., Chen, J., McCarthy, K. D., 2007. Selective stimulation of astrocyte calcium in situ does not affect neuronal excitatory synaptic activity. Neuron 54, 611-626.

Fiacco, T. A., McCarthy, K. D., 2018. Multiple Lines of Evidence Indicate That Gliotransmission Does Not Occur under Physiological Conditions. J Neurosci 38, 3-13.
Goette, L., Bendahan, S., Thoresen, J., Hollis, F., Sandi, C., 2015. Stress pulls us apart: anxiety leads to differences in competitive confidence under stress. Psychoneuroendocrinology 54, 115-123.

Gordon, G. R., Baimoukhametova, D. V., Hewitt, S. A., Rajapaksha, W. R., Fisher, T. E., Bains, J. S., 2005. Norepinephrine triggers release of glial ATP to increase postsynaptic efficacy. Nat Neurosci 8, 1078-1086.

Halassa, M. M., Haydon, P. G., 2010. Integrated brain circuits: astrocytic networks modulate neuronal activity and behavior. Annu Rev Physiol 72, 335-355.

Hollis, F., Mitchell, E. S., Canto, C., Wang, D., Sandi, C., 2018. Medium chain triglyceride diet reduces anxiety-like behaviors and enhances social competitiveness in rats. Neuropharmacology 138, 245-256.

Hollis, F., van der Kooij, M. A., Zanoletti, O., Lozano, L., Cantó, C., Sandi, C., 2015. Mitochondrial function in the brain links anxiety with social subordination. Proceedings of the National Academy of Sciences 112, 15486-15491.

Holmstrom, M. H., Iglesias-Gutierrez, E., Zierath, J. R., Garcia-Roves, P. M., 2012. Tissue-specific control of mitochondrial respiration in obesity-related insulin resistance and diabetes. American Journal of Physiology-Endocrinology and Metabolism 302, E731-E739.

Larrieu, T., Cherix, A., Duque, A., Rodrigues, J., Lei, H., Gruetter, R. and Sandi, C., 2017. Hierarchical status predicts behavioral vulnerability and nucleus accumbens metabolic profile following chronic social defeat stress. *Current Biology*, *27*(14), pp.2202-2210.

Li, X. D., Zima, A. V., Sheikh, F., Blatter, L. A., Chen, J., 2005. Endothelin-1-induced arrhythmogenic Ca2+ signaling is abolished in atrial myocytes of inositol-1,4,5-trisphosphate(IP3)-receptor type 2-deficient mice. Circulation Research 96, 1274-1281.

Magistretti, P. J., Allaman, I., 2015. A cellular perspective on brain energy metabolism and functional imaging. Neuron 86, 883-901.

Marpegan, L., Swanstrom, A.E., Chung, K., Simon, T., Haydon, P.G., Khan, S.K., Liu, A.C., Herzog, E.D. and Beaulé, C., 2011. Circadian regulation of ATP release in astrocytes. *Journal of Neuroscience*, *31*(23), pp.8342-8350.

Mergenthaler, P., Lindauer, U., Dienel, G. A., Meisel, A., 2013. Sugar for the brain: the role of glucose in physiological and pathological brain function. Trends Neurosci 36, 587-597.

Morris, R. G. M., 1981. Spatial Localization Does Not Require the Presence of Local Cues. Learning and Motivation 12, 239-260.

Navarrete, M., Perea, G., Fernandez de Sevilla, D., Gomez-Gonzalo, M., Nunez, A., Martin, E. D., Araque, A., 2012. Astrocytes mediate in vivo cholinergic-induced synaptic plasticity. PLoS Biol 10, e1001259.

Newman, E. A., 2003. Glial cell inhibition of neurons by release of ATP. J Neurosci 23, 1659-1666.

Okubo, Y., Kanemaru, K., Suzuki, J., Kobayashi, K., Hirose, K. and Iino, M., 2019. Inositol 1, 4, 5-trisphosphate receptor type 2-independent Ca2+ release from the endoplasmic reticulum in astrocytes. *Glia*, *67*(1), pp.113-124.

Oliveira, J.F., Sardinha, V.M., Guerra-Gomes, S., Araque, A. and Sousa, N., 2015. Do stars govern our actions? Astrocyte involvement in rodent behavior. *Trends in neurosciences*, *38*(9), pp.535-549.

Pascual, O., Casper, K. B., Kubera, C., Zhang, J., Revilla-Sanchez, R., Sul, J. Y., Takano, H., Moss, S. J., McCarthy, K., Haydon, P. G., 2005. Astrocytic purinergic signaling coordinates synaptic networks. Science 310, 113-116.

Petravicz, J., Boyt, K. M., McCarthy, K. D., 2014. Astrocyte IP3R2-dependent Ca(2+) signaling is not a major modulator of neuronal pathways governing behavior. Front Behav Neurosci 8, 384.

Petravicz, J., Fiacco, T. A., McCarthy, K. D., 2008. Loss of IP3 receptor-dependent Ca2+ increases in hippocampal astrocytes does not affect baseline CA1 pyramidal neuron synaptic activity. J Neurosci 28, 4967-4973.

Picard, M., McEwen, B. S., Epel, E. S., Sandi, C., 2018. An energetic view of stress: Focus on mitochondria. Front Neuroendocrinol 49, 72-85.

Rangaraju, V., Calloway, N., Ryan, T. A., 2014. Activity-driven local ATP synthesis is required for synaptic function. Cell 156, 825-835.

Sapolsky, R. M., 2005. The influence of social hierarchy on primate health. Science 308, 648-652.

Savtchouk, I., Volterra, A., 2018. Gliotransmission: Beyond Black-and-White. J Neurosci 38, 14-25.

Serrano, A., Haddjeri, N., Lacaille, J. C., Robitaille, R., 2006. GABAergic network activation of glial cells underlies hippocampal heterosynaptic depression. J Neurosci 26, 5370-5382.

Srinivasan, R., Huang, B. S., Venugopal, S., Johnston, A. D., Chai, H., Zeng, H., Golshani, P., Khakh, B. S., 2015. Ca(2+) signaling in astrocytes from Ip3r2(-/-) mice in brain slices and during startle responses in vivo. Nat Neurosci 18, 708-717.

Suzuki, A., Stern, S. A., Bozdagi, O., Huntley, G. W., Walker, R. H., Magistretti, P. J., Alberini, C. M., 2011. Astrocyte-neuron lactate transport is required for long-term memory formation. Cell 144, 810-823.

Takata, N., Nagai, T., Ozawa, K., Oe, Y., Mikoshiba, K., Hirase, H., 2013. Cerebral blood flow modulation by Basal forebrain or whisker stimulation can occur independently of large cytosolic Ca2+ signaling in astrocytes. PLoS One 8, e66525.

van der Kooij, M. A., Hollis, F., Lozano, L., Zalachoras, I., Abad, S., Zanoletti, O., Grosse, J., Guillot de Suduiraut, I., Canto, C., Sandi, C., 2018. Diazepam actions in the VTA enhance social dominance and mitochondrial function in the nucleus accumbens by activation of dopamine D1 receptors. Mol Psychiatry 23, 569-578.

Volterra, A., Liaudet, N., Savtchouk, I., 2014. Astrocyte Ca(2)(+) signalling: an unexpected complexity. Nat Rev Neurosci 15, 327-335.

Volterra, A., Meldolesi, J., 2005. Astrocytes, from brain glue to communication elements: the revolution continues. Nat Rev Neurosci 6, 626-640.

Wang, F., Smith, N. A., Xu, Q., Fujita, T., Baba, A., Matsuda, T., Takano, T., Bekar, L., Nedergaard, M., 2012. Astrocytes modulate neural network activity by Ca(2)+-dependent uptake of extracellular K+. Sci Signal 5, ra26.

Wang, F., Zhu, J., Zhu, H., Zhang, Q., Lin, Z., Hu, H., 2011. Bidirectional control of social hierarchy by synaptic efficacy in medial prefrontal cortex. Science 334, 693-697.

Womac, A.D., Burkeen, J.F., Neuendorff, N., Earnest, D.J. and Zoran, M.J., 2009. Circadian rhythms of extracellular ATP accumulation in suprachiasmatic nucleus cells and cultured astrocytes. *European Journal of Neuroscience*, *30*(5), pp.869-876.

Zhang, J. M., Wang, H. K., Ye, C. Q., Ge, W., Chen, Y., Jiang, Z. L., Wu, C. P., Poo, M. M., Duan, S., 2003. ATP released by astrocytes mediates glutamatergic activity-dependent heterosynaptic suppression. Neuron 40, 971-982.

Zhou, T., Sandi, C., Hu, H., 2018. Advances in understanding neural mechanisms of social dominance. Curr Opin Neurobiol 49, 99-107.

Zhou, T., Zhu, H., Fan, Z., Wang, F., Chen, Y., Liang, H., Yang, Z., Zhang, L., Lin, L., Zhan, Y., Wang, Z., Hu, H., 2017. History of winning remodels thalamo-PFC circuit to reinforce social dominance. Science 357, 162-168.

Figure Legends

Figure 1. There are no differences in anxiety or exploratory behavior between wildtype and IP3R2-/- mice. (A) Representative wildtype (WT) and IP3R2-/- (KO) heatmaps of the elevated plus maze (EPM) show similar levels of activity between genotypes. (B) There were no significant differences between genotypes in the time spent in the anxiogenic open arms (Mann-Whitney test, U=88.5; p=0.48); (C) number of entries to the open arms (Unpaired t-test; t=0.78; p=0.45); (D) or distance traveled in the maze (Unpaired t-test, t=0.22; p=0.82). (E) Representative WT and KO heatmaps of the open field test show similar patterns of behavior between genotypes. (F) There were no significant differences between WT and KO mice in the percentage of time spent in the center (Mann-Whitney test, U=90; p=0.53); (G) number of entries to the center of the field (Unpaired t-test, t=0.86, p=0.40); (H) or distance moved (Unpaired t-test, t=0.75, p=0.46). n=14-15/group.

Figure 2. IP3R2-/- and wildtype mice have similar probabilities to become dominant in the dominance tube test. (A) Scheme demonstrating the dominance tube test, where two mice are paired and placed inside the tube such that they meet in the middle. The dominant mouse is the one who pushes the other mouse out of the tube. (B) Across all sessions, there were no significant differences between wildtype (WT) and IP3R2-/- (KO) mice in the number of trials won (one-sample t-test t=0.59; df=13; *p*=0.57). (C) There were no significant effects of genotype (RM-ANOVA, F(1,26)= 0.69; p=0.41), time (F(2,52)= 0.0004; p=0.99) or an interaction (Figure 2C; F(2,52)= 2; p=0.15) in dominance behavior across each of the three testing days. (D) Dominant mice overall became faster at asserting their dominance across the three testing days (F(8,48)= 4.51; p = 0.0004). While there was no effect of genotype (F(1,6)= 0.66; p =0.44), there was a significant interaction between genotype and day (F(8,48)= 5.05; p= 0.0001) such that KO mice took longer to assert their dominance on the first day only (Day 1 trial 1: WT vs KO p =0.0098). n=14 WT-KO pairs.

Figure 3. IP3R2-/- mice have similar levels of mitochondrial respiration in the nucleus accumbens and prefrontal cortex. (A) Wildtype (WT) and IP3R2-/- (KO) mice had similar levels of mitochondrial respiration in the nucleus accumbens for both coupled (CI: (F(1,23)=0.242; *p*=0.63, CI+CII: F(1,23.2)=0.204; *p*=0.67) and uncoupled (ETS: F(1,23.2)=0.080; *p*=0.78, ETSCII: F(1,23.2)= 0.68; *p*=0.42) respiration. (B) Similarly, there were no significant differences in coupled (CI: F(1,24.3)= 0.725 *p*=0.40, CI+CII: F(1,24.04)= 0.645; *p*=0.43; n=14-15/group) or uncoupled (ETS: F(1,22.57)= 0.397; *p*=054, ETSCII; F(1,24.01)= 0.162; *p*=1.0) respiration in the medial prefrontal cortex between WT and KO mice. N=14-15/group.

Figure 4. No effect of astrocytic ATP release through IP_3R2 on learning and memory in the Morris Water Maze. (A) There were no significant differences in the latency to escape to the platform during training between genotypes (F(1, 12) = 0.3561; p=0.56), with both genotypes learning the task across time for both the acquisition (F(18, 216) = 7.967; p<0.0001) and reversal (F(11, 132) = 10.45; p<0.0001). (B) Representative heatmaps of WT (top) and KO (bottom) in the Morris Water Maze during the probe trial show similar patterns of behavior. (C) WT and KO mice both spent significantly more time in the platform zone than chance levels (WT: t=7.37 df=6; p=0.0002; KO: t= 4.81, df=6; p=0.003) to a similar degree (t= 0.125; df=12; p= 0.90). (D) During the reversal probe, mice spent similar amounts of time in the new platform

zone as chance levels would predict (t=0.03632 df=6; p=0.97), with no difference between genotypes (t=0.01948 df=12; p=0.98). (E) Coupled (CI: F(1,8.9)=2.6; p=0.14; CI+CII: F(1,8.9)=2.8; p=0.13) and uncoupled (ETS: F(1,8.9)=3.1; p=0.11; ETSCII: F(1,8.9)=2.4; p=0.16) mitochondrial respiration under basal conditions in the hippocampus was not significantly different between WT and KO mice. n= 7/group for behavior; n=4-9/group for respiration.

Figure 5. No behavioral or mitochondrial differences when tested during circadian night. All experiments were performed during the dark phase at peak astrocytic ATP release. (A) There were no significant differences in the percentage of time spent in the open arms Mann-Whitney test, U=32; p>0.99), (B) number of entries (unpaired t-test; t=1.08; df=14; *p*=0.30) or (C) distance traveled (unpaired t-test; t=0.67; df=14; *p*=0.52) in the elevated plus maze between WT and KO littermates. (D) *IP_3R2-/-* animals exhibited an equal probability to become dominant (one-sample t-test t=0.23; df=7; *p*=0.84; n=8 WT-KO pairs), (E) with no significant effect of genotype (F(1,14)=0.082; *p*=0.78), time (F(1.82, 25.5)=1.06e-12; p>0.99) or an interaction in the number of trials won (F(2,28)=0.64; *p*=0.53) and (F) no significant differences in the time to exert dominance between dominant KO and WT mice at the genotype (F1,6)=1.69; *p*=0.24), time (F(2.2, 13.7)=2.1; *p*=0.16), or interaction (F(8,48)=1.4; *p*=0.21) levels (n=4/group). WT and KO animals exhibited similar mitochondrial respiration in the (G) nucleus accumbens (CI: F(1,11)=0.004; *p*=0.95; CI+CII: F(1,14)=0.064; *p*=0.80; ETS: F(1,14)=0.024; *p*=0.88 ETSCII: F(1,14)=0.026; *p*=0.88), (H) prefrontal cortex (CI: F(1,11)=0.34; *p*=0.57; CI+CII: F(1,11)=0.016; *p*=0.90; ETS: F(1,11)=0.56; *p*=0.47; ETSCII: F(1,11)=0.29; *p*=0.60), and (I) hippocampus (CI: F(1,11)=0.69; *p*=0.43; CI+CII: F(1,11)=0.74; *p*=0.41; ETS: F(1,11)=0.61; *p*=0.45; ETSCII: F(1,11)=0.88; *p*=0.37). WT and KO animals also exhibited similar levels of ATP in the (J) prefrontal cortex (F(1,11)=2.1; *p*=0.18), (K) nucleus accumbens (F(1,14)=0.086; *p*=0.77) or (L) hippocampus (F(1,9.9)=1.34; *p*=0.27). N=8/group except when specified otherwise.

Figure 1

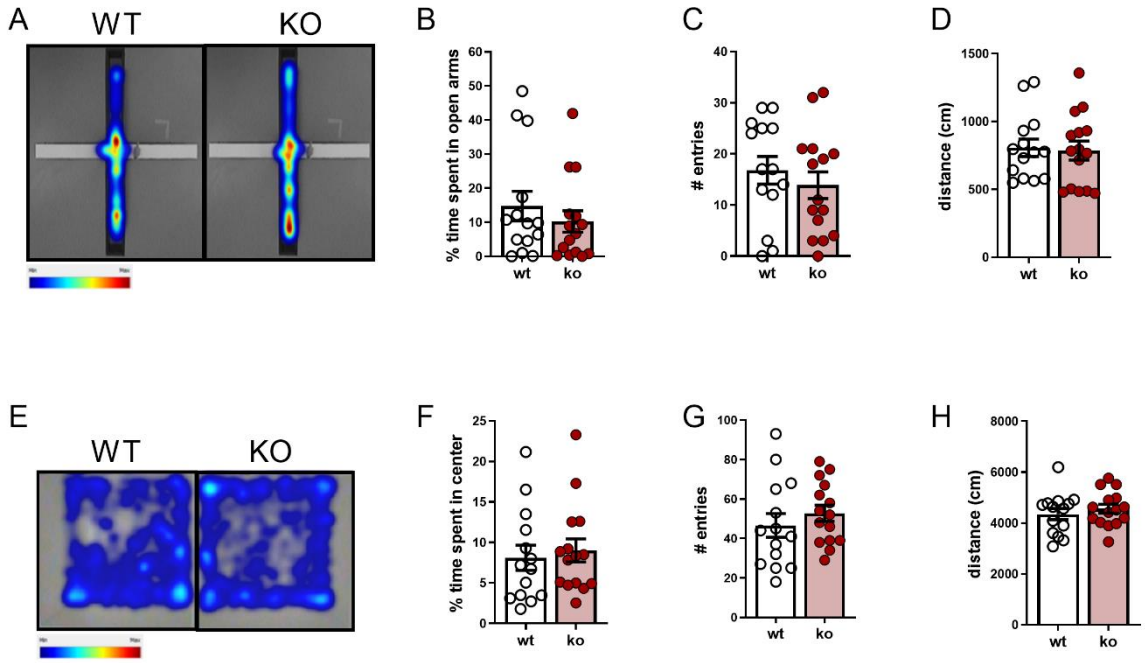
A
WT
KO
B
% time spent in open arms
wt
ko
C
entries
wt
ko
D
distance (cm)
wt
ko
E
WT
KO
F
% time spent in center
wt
ko
G
entries
wt
ko
H
distance (cm)
wt
ko

Figure 2

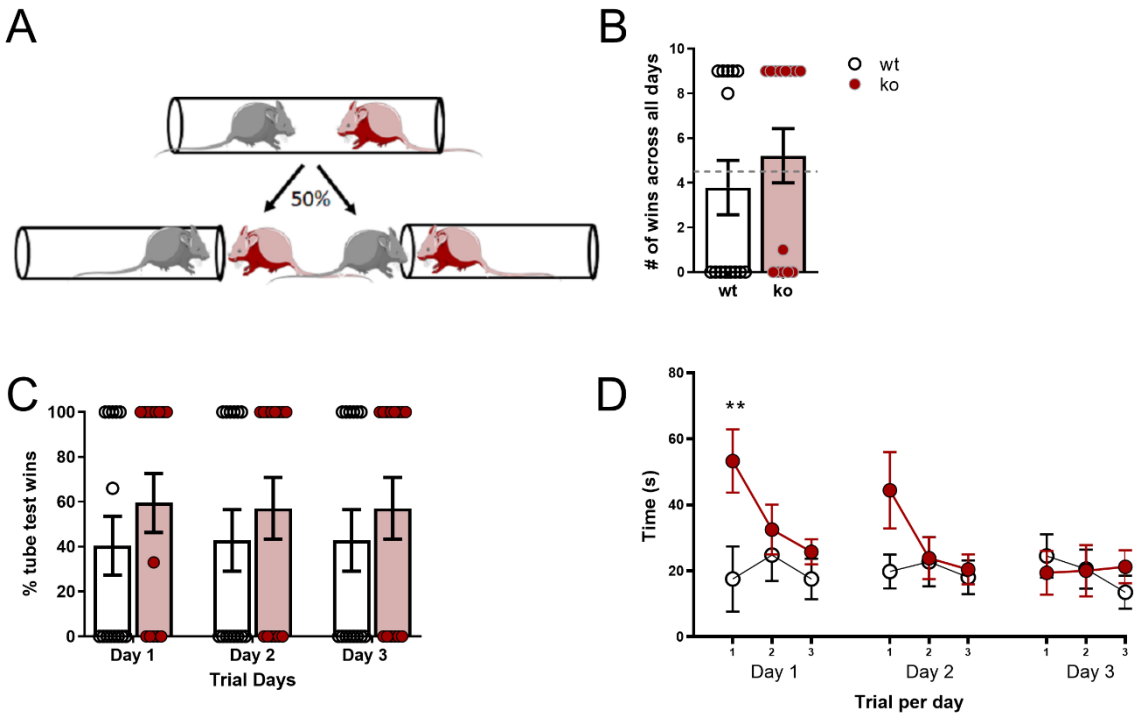
A
50%
B
# of wins across all days
wt
ko
C
% tube test wins
Day 1
Day 2
Day 3
Trial Days
D
Time (s)
**
Day 1
Day 2
Day 3
Trial per day

Figure 3

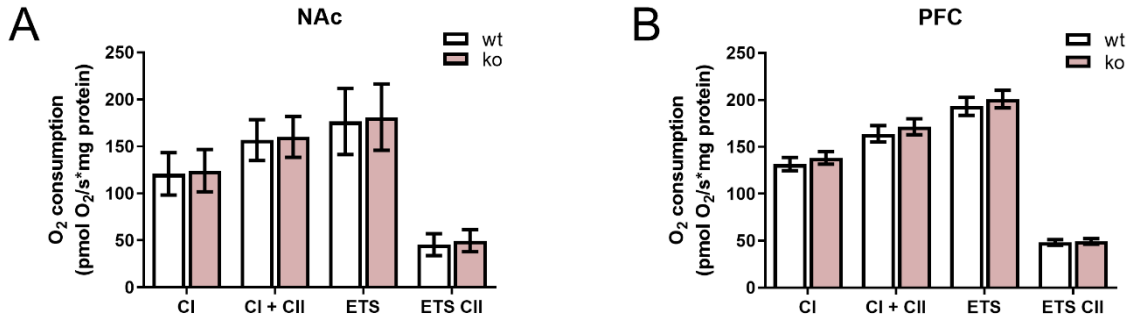
A
NAc
wt
ko
O2 consumption (pmol O2/s*mg protein)
250
200
150
100
50
0
CI
CI + CII
ETS
ETS CII
B
PFC
wt
ko
O2 consumption (pmol O2/s*mg protein)
250
200
150
100
50
0
CI
CI + CII
ETS
ETS CII

Figure 4

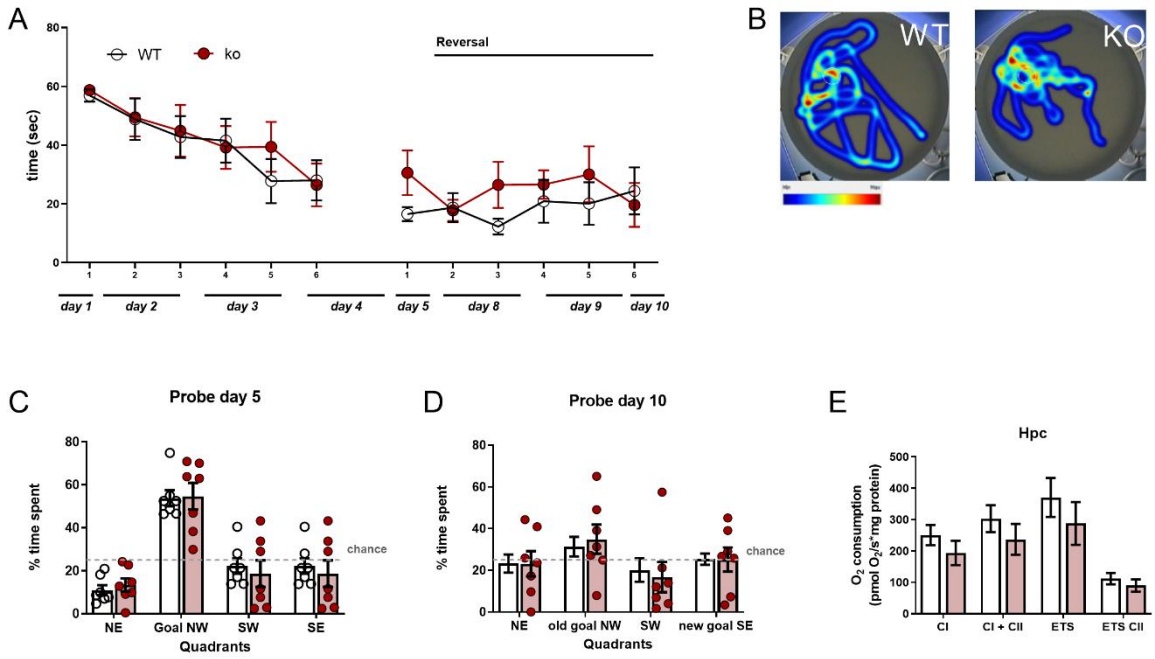
A
WT
ko
Reversal
time (sec)
day 1
day 2
day 3
day 4
day 5
day 8
day 9
day 10
B
WT
KO
C
Probe day 5
% time spent
chance
NE
Goal NW
SW
SE
Quadrants
D
Probe day 10
% time spent
chance
NE
old goal NW
SW
new goal SE
Quadrants
E
Hpc
O2 consumption (pmol O2/s*mg protein)
CI
CI + CII
ETS
ETS CII

Figure 5

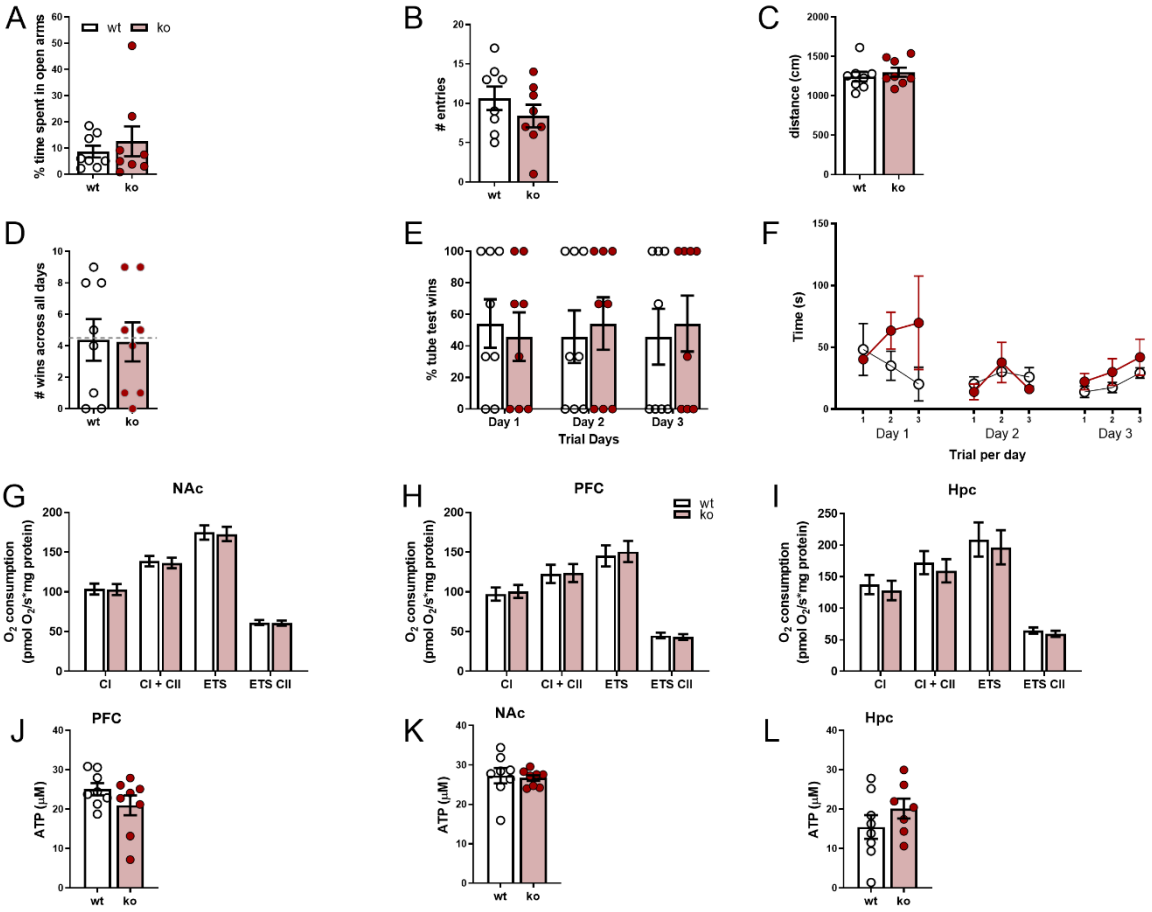
A
wt
ko
% time spent in open arms
B
entries
C
distance (cm)
D
wins across all days
E
% tube test wins
Day 1
Day 2
Day 3
Trial Days
F
Time (s)
Trial per day
G
NAc
H
PFC
I
Hpc
O2 consumption (pmol O2/s*mg protein)
CI
CI + CII
ETS
ETS CII
J
PFC
K
NAc
L
Hpc
ATP (µM)